Available online at www.sciencedirect.com
ScienceDirect
Journal of Photochemistry and Photobiology A: Chemistry 189 (2007) 205–210
Journal of Photochemistry and Photobiology A:Chemistry
www.elsevier.com/locate/jphotochem

SAC-CI theoretical study on the excited states of lumiflavin: Structure, excitation spectrum, and solvation effect

Jun-ya Hasegawa [a,b], Sareeya Bureekaew [a], Hiroshi Nakatsuji [a,b,*]

[a] *Department of Synthetic Chemistry and Biological Chemistry, Graduate School of Engineering, Kyoto University, Kyoto-Daigaku-Katsura, Nishikyo-ku, Kyoto 615-8510, Japan*
[b] *Quantum Chemistry Research Institute (QCRI), 58-8 Mikawa, Momoyama-cho, Fushimi-ku, Kyoto 612-8029, Japan*

Received 4 November 2006; received in revised form 31 January 2007; accepted 31 January 2007
Available online 3 February 2007

Abstract

The excited states of a flavin-related compound, lumiflavin, were studied by the symmetry-adapted cluster (SAC)-configuration interaction (CI) method. The absorption peaks observed in the experimental spectrum were theoretically assigned. Transition energy of some low-lying n–π* states were obtained. The energy minimum structures of the first singlet and triplet excited states were calculated by the SAC-CI method. The structural changes upon excitation were at most 0.05 Å. The solvation effect on the absorption energy in aqueous solution was investigated using polarizable continuum model (PCM) and by including water molecules into the computational model. The solvatochromic shift of the second peak ($3^1A'$ state) originates from both microscopic (hydrogen bonding) and macroscopic (electronic polarization of solvent) solvation effects.

Keywords: Lumiflavin; Excited state; SAC-CI method; Structure; Solvatochromism

1. Introduction

Flavins are well-known redox-active chromophores that are widely found in enzymes and photoreceptors [1]. These compounds contain a heterocyclic isoalloxazine ring (7,8-dimethyl benzo[*g*]pteridine-2,4(3*H*,10*H*)-dione) that exhibits electron-transfer capability. Riboflavin is found in various types of foods in the human diet. A lack of riboflavin causes growth disturbance, skin disease, and hair loss. Flavin adenine dinucleotide (FAD) works as a redox-active light-harvesting chromophore in DNA photolyase, blue-light-using FAD (BLUF), and cryptochrome. Flavin mononucleotide (FMN) exhibits redox-active properties in respiratory complex I in mitochondria and other electron-transfer systems. FMN also functions as a blue light photoreceptor in phototropin.

Since flavins play important roles in a very wide range of biological processes in which both ground and excited states of theses molecules are involved, their photophysical and photochemical properties have been studied from various points of view [2–11]. Lumiflavin (LF), which is shown in Fig. 1a, is one of the simplest flavin compounds. In ongoing efforts to study photoexcitation and electron-transfer reactions in flavin-type compounds, LF has been used as a representative molecule. Several studies on electronic excitation of LF have been published, involving both experimental research [2,4,7–11] and theoretical calculations [3,5–11]. Theoretical studies using configuration interaction-singles (CIS) [6], time-dependent density functional theory (TDDFT) [6,8–10] and DFT-multireference (MR) CI [6] have been reported. These studies mainly focused on the excitation spectrum. A complete active space self-consistent field method with second-order perturbation theory (CASPT2) study [3] on the excited states of isoalloxazine has recently been published. This study reported the ground-state absorption spectrum and the potential energy surface of the low-lying singlet

Abbreviations: SAC-CI method, symmetry-adapted cluster-configuration method; PCM, polarizable continuum model; CIS, configuration interaction-singles; TDDFT, time-dependent density functional theory; MR-CI, multi-reference CI; CASPT2, complete active space self-consistent field method with second-order perturbation theory; CASSCF, complete active space self-consistent field method; HOMO, highest-occupied molecular orbital; LUMO, lowest-unoccupied molecular orbital

* Corresponding author at: Department of Synthetic Chemistry and Biological Chemistry, Graduate School of Engineering, Kyoto University, Kyoto-Daigaku-Katsura, Nishikyo-ku, Kyoto 615-8510, Japan. Tel.: +81 75 383 2738; fax: +81 75 383 2741.
E-mail address: hiroshi@sbchem.kyoto-u.ac.jp (H. Nakatsuji).

1010-6030/$ – see front matter © 2007 Elsevier B.V. All rights reserved.
doi:10.1016/j.jphotochem.2007.01.033

and triplet states. Photochemical events in the gas phase was interpreted using a quantitative correlated method. Since LF is a trimethyl-isoalloxazine, important problems regarding the excited states of LF in the gas phase might have been solved. However, these studies on LF failed to reproduce the excitation energy for the second peak, and its maximum error reached 0.5 eV [6]. One of the remaining problems is to clarify the reason why the absorption energy of the second peak has never been reproduced quantitatively, even though modern correlated methods have been employed. One of the main reasons is the solvation effect on the excitation energy. In general, the absorption energy of the π–π* transition does not strongly depend on the solvent. However, the second peak shifts by approximately 0.4 eV by the solvation effect. The above-mentioned studies did not include the solvation effect in their computations.

In this study, we applied the symmetry-adapted cluster (SAC) [12]/SAC-configuration interaction (CI) [13–15] method [16,17]. The SAC/SAC-CI method is established as an accurate electron-correlation method for studying ground, excited, ionized and electron-attached states. As numerous applications have shown, the SAC-CI method is a reliable tool for calculating the excitation energy and properties of excited states of molecules[16,17]. In the present report, we first show SAC-CI results for the excited states of LF in the gas phase. The optimized structures are explained in some details for ground, singlet, and triplet excited states at the SAC/SAC-CI level. Next we investigated the solvation effect in the excited states. As a previous experimental study showed [8], the excitation energy of the second peak remarkably depends on the solvent, even though the absorption was assigned to a π–π* transition. We applied the polarizable continuum model (PCM) [18–20] to the SAC-CI calculations to capture the solvation effect. With these calculations, we succeeded in explaining the solvent dependent excitation energy observed in the second peak.

2. Computational details

The computational models for LF are shown in Fig. 1. The isolated model (Fig. 1a) was used for the gas-phase calculations. The second model with five water molecules (Fig. 1b) was used to investigate the effect of hydrogen bondings in water solution.

The geometry of LF in the gas phase was optimized by density functional theory (DFT) [21–23] using the B3LYP [24,25] functional. The structure of LF with five water molecules was also optimized using DFT calculations. The optimized geometries were confirmed to be the energy-minimum by performing frequency analysis. The optimized structure has C_s symmetry, which agrees with previous studies [3,26]. The 6-31G(d) [27,28] basis sets were used for both LF and water molecules. We also performed geometry optimization for the ground (S_0), the first singlet (S_1), and triplet (T_1) excited states by using the SAC/SAC-CI method with D95V(d) basis functions [29]. We performed the SAC-CI optimization within the C_s symmetry. To date, the second derivative of the SAC-CI energy has not yet been developed. We referred to recently published complete active space self-consistent field method (CASSCF) structures for the S_1 and T_1 states, which are found to be planar (C_s-symmetry) in both cases [3].

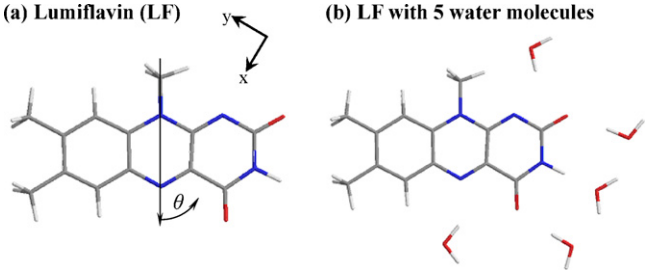

Fig. 1. Computational models for (a) lumiflavin (LF) and (b) lumiflavin with five explicit water molecules directly solvating the charged atoms. The arrays in (a) show the definition of the angle (θ) of the transition dipole moment vector.

The solvation effect in water solution was included using the PCM [18–20]. The dielectric constant of water ($\varepsilon = 78.39$) was used. For the model with five water molecules, the rest of the solvation effect was treated using the PCM. The self-consistent reaction field calculation was performed at the ground-state Hartree-Fock (HF) level, and the orbitals and one-electron operators were transferred to the SAC/SAC-CI calculation.

For the SAC/SAC-CI calculations, we employed the D95V(d) sets. The 1s orbitals of C, N, and O atoms were treated as frozen-core orbitals. The active orbitals were comprised of 48 occupied orbitals and 223 virtual orbitals. All the single and selected double excitation operators were included in the SAC/SAC-CI wave functions. Perturbation selection [30] was performed to select the important doubles. The energy thresholds for the perturbation selection procedure were 5.0×10^{-6} and 5.0×10^{-7} a.u. for the ground and excited states, respectively. The oscillator strengths reported in this paper were calculated in dipole length representation. All computations were carried out using the Gaussian 03 quantum chemistry program package [31].

3. Results and discussion

3.1. Electronic excitation of lumiflavin in the gas phase

We begin with the electronic excitation spectrum for the ground state of LF in the gas phase. The SAC-CI results are summarized in Table 1. Unfortunately, there is no experimental gas-phase spectrum available for comparison. In solution, LF shows the first band centered at 2.77–2.81 eV, depending on the solvent [8]. On the low-energy side of the absorption peak, there is also a strong shoulder at 2.6 eV. In the SAC-CI result, the first singlet excited state ($2^1A'$) was calculated at 2.46 eV. There is a deviation of 0.14 eV from the shoulder and of 0.31–0.35 eV from the peak center. Since there is no other excited state in this energy region of the spectrum, the $2^1A'$ state is assigned to the first band. The S_1 state is characterized as a π–π* transition dominated by HOMO-LUMO transition. Fig. 2 shows some important MOs. Both HOMO and LUMO are delocalized over the π skeleton of the ring. Using linear dichroism (LD) spectroscopy, the angle of the transition dipole moment in FMN [32,33] was measured. The definition of the angle (θ) is indicated in Fig. 1a. Johansson et al. [33] and Eaton et al. [32]

Table 1
Excited states of lumiflavin calculated by the SAC-CI method

State	SAC-CI						Expt.[c]					
	Nature	Main configuration	E_{ex} (Osc.)[a]			LD[b]	E_{ex}[a]					LD[b]
			In gas phase	In water solution			in Dx[e] $\varepsilon = 4.03$	in DCE[f] $\varepsilon = 10.36$	in MeOH[g] $\varepsilon = 32.63$	in AcN[h] $\varepsilon = 36.64$	in H_2O[i] $\varepsilon = 78.39$	
				PCM	$5H_2O$[d]	θ (°)						θ (°)
$2^1A'$	$\pi-\pi^*$	$67 \rightarrow 68$	2.46 (0.0909)	2.42 (0.1767)	2.40	72.0	(−/2.81[j])	(−/2.77[j])	(2.6[j]/2.80[j])	(2.6[j]/2.80[j])	(2.6[k]/2.79[j], 2.78[k])	$58 \pm 4, 75$
$1^1A''$	$n-\pi^*$	$63 \rightarrow 68$	3.18 (0.0018)	3.38 (0.0017)	3.28							
$2^1A''$	$n-\pi^*$	$62 \rightarrow 68$	3.59 (0.0001)	4.12 (0.0001)	4.05							
$3^1A'$	$\pi-\pi^*$	$66 \rightarrow 68$	3.84 (0.1455)	3.56 (0.1769)	3.54	85.0	3.73[j]	3.59[j]	3.53[j]	3.62[j]	3.38[j], 3.35[k]	$97 \pm 3, 95$
$4^1A'$	$\pi-\pi^*$	$67 \rightarrow 69$	4.55 (0.0759)	4.57 (0.2188)	4.56	108.0	–	–	4.65[l]	4.65[l]	4.59[k]	119 ± 2
$5^1A'$	$\pi-\pi^*$	$67 \rightarrow 70$	4.86 (0.2125)	4.96 (0.3471)	4.95	125.0						

[a] Excitation energy in eV. Numbers in parentheses are the oscillator strength in atomic units.
[b] Angle of the transition dipole moment from LD data. The definition of the angle is shown in Fig. 1a.
[c] Experimental absorption energy. The data (x/y) for the $2^1A'$ state denotes that the strong shoulder is at "x" eV and the peak maximum at "y" eV.
[d] Effect of the explicit hydrogen bonds using the $5H_2O$ model was taken into account. Correction to the SAC-CI excitation energy was obtained by the ONIOM like procedure at CIS level.
[e] In 1,4-dioxane solution.
[f] In dichloroethane solution.
[g] In methanol solution.
[h] In acetonitrile solution.
[i] In water solution.
[j] Ref. [8].
[k] Ref. [6].
[l] Ref. [10].

reported $\theta = 58° \pm 4°$ and 75°, respectively. The present SAC-CI result is 72°, which is very close to the CASPT2 result for isoalloxane (75°) [3]. The theoretical results thus support the latter experiment.

There are two (n + σ)–π* states around 3.2–3.6 eV. The $1^1A''$ and $2^1A''$ states calculated at 3.18 and 3.59 eV are transitions from HOMO-4 to LUMO and from HOMO-5 to LUMO, respectively. The n + σ orbitals HOMO-4 and HOMO-5 are characterized as mixed σ and lone-pair O (n_O) and N (n_N) orbitals. HOMO-4 has a relatively larger orbital amplitude at the nitrogen atoms, while that of HOMO-5 is at the oxygen atoms.

The second π–π* transition, the $3^1A'$ state, is at 3.84 eV in the SAC-CI result for the gas phase. The corresponding experimental peak position ranges from 3.73 to 3.38 eV, depending on the solvent [3]. The most non-polar and aprotic solvent used in the experiment was 1,4-dioxane. In this solution, the peak was observed at 3.73 eV. The main configuration of the state is a transition from HOMO-1 to LUMO. As observed in Fig. 2d, HOMO-1 has a population around the left ring. Table 2 summarizes the calculated dipole moments of the ground and low-lying π–π* states. The total dipole moment of the $3^1A'$ state is 13.2 Debye, which is greater than those of the ground and $2^1A'$ states by 3.6 and 2.0 Debye, respectively. Compared to the ground state, the Cartesian components μ_x and μ_y increase by 1.8 and 3.3 Debye, respectively. This change is related to the main configuration of the state. Owing to the localized character of HOMO-1, the charger-transfer character of the $3^1A'$ state is greater than that of the $2^1A'$ state. As mentioned later, this property becomes important for interpreting the solvent dependence of the absorption peak. The angle of the transition dipole moment was calculated to be 85.0°. The experimental values obtained by LD spectroscopy were $97° \pm 3°$ by Johansson et al. [33] and 95° by Eaton et al. [32], which are in reasonable agreement with the present value and the CASPT2 result [3] (100°).

For the third and fourth π–π* transitions, the $4^1A'$ and $5^1A'$ states were calculated at 4.55 and 4.86 eV, respectively, in the present SAC-CI result. The main configurations of the $4^1A'$ and $5^1A'$ states are transitions from HOMO to LUMO+1 and from HOMO to LUMO+2, respectively. In the experimental spectrum, there is a broad absorption peak centered at approximately 4.5 eV. Considering the absorption coefficient in the experimental spectrum, both the $4^1A'$ and $5^1A'$ states would contribute to this absorption. The angle of the transition dipole moment calculated is 108.0° and 125.0° for these states, respectively. On the other hand, the experimental value for the peak is $119° \pm 2°$

Table 2
Dipole moment of ground, $2^1A'$ and $3^1A'$ states in the gas phase calculated by the SAC-CI method

State	Dipole moment (Debye)			
	μ_x	μ_y	μ_z	μ_{tot}
X^1A' (ground state)	3.0	9.1	0.0	9.6
$2^1A'$ (HOMO → LUMO)	2.6	10.9	0.0	11.2
$3^1A'$ (HOMO-1 → LUMO)	4.8	12.4	0.0	13.3

Definitions of the x- and y-axes are indicated in Fig. 1a.

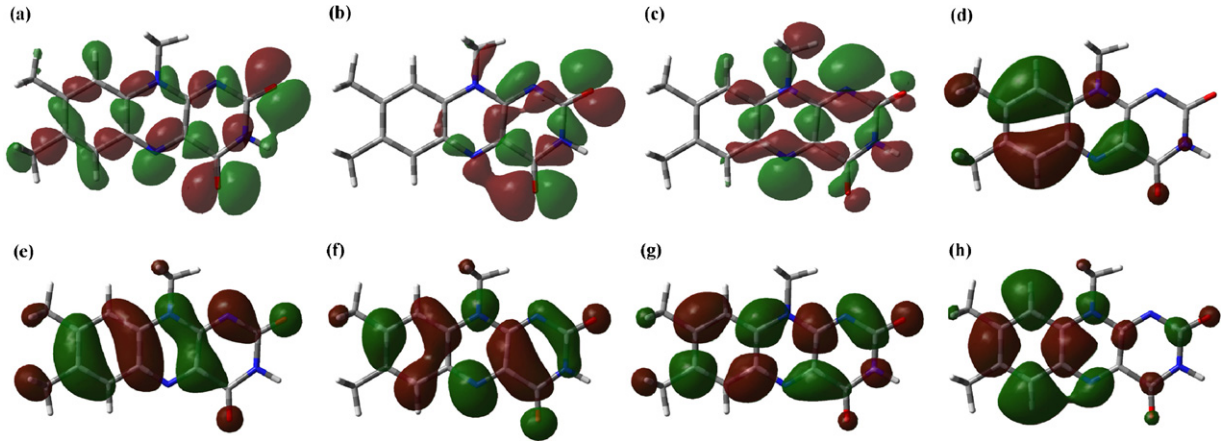

Fig. 2. Hartree-Fock molecular orbitals of lumiflavin in the gas phase. These orbitals are relevant to the low-lying excited states: (a) 60th MO (n+σ, HOMO-7); (b) 62th MO (n+σ, HOMO-5); (c) 63th MO (n+σ, HOMO-4); (d) 66th MO (π, HOMO-1); (e) 67th MO (π, HOMO); (f) 68th MO (π, LUMO); (g) 69th MO (π, LUMO+1); (h) 70th MO (π, LUMO+2).

[33]. Therefore, the angle averaged for the two states is close to the experimental value.

3.2. Structure of LF in the lowest singlet and triplet excited states (S_1 and T_1)

The structures of LF in the S_1 ($2^1A'$) and T_1 ($1^3A'$) states in the gas phase were determined by the SAC-CI method. The optimized bond lengths are summarized in Fig. 3. The result for the ground state (S_0) is also shown in Fig. 3a. Both states were characterized as a HOMO (π) to LUMO (π*) transition. As shown in Fig. 3, the transitions cause no significant change in the bond lengths. The maximum change is at most 0.05 Å, observed for the C8–C9, C4–C5, and C4–C7 bonds. The reason can be found in the nature of the HOMO and LUMO. There is no clear bonding to anti-bonding transition in the HOMO–LUMO excited state. The transition is mostly from the bonding to non-bonding orbitals and from the anti-bonding to non-bonding orbitals. The changes in the bond lengths reflect the character of the HOMO and LUMO. For example, the C4–C5 bond has bonding character in the HOMO, while it changes to non-bonding in the LUMO. The C4–C5 bond lengthens in the first excited state. The C8–C11 bond shortens in both the S_1 and T_1 states, because the LUMO shows bonding character for the C8–C11 bond, which is stronger than that of the HOMO.

3.3. Solvation effect on the excitation energy of the singlet states

The present gas-phase result shows reasonable agreement to the experimental absorption energy in 1,4-dioxane solution [8], which is the most non-polar and aprotic solvent of those used in experiments. Since previous theoretical studies were on the excited states of LF in the gas phase [3,6,8,9,11], one of the problems to be solved is the absorption energy in polar and protic solution. In particular, the absorption energy of the second peak strongly depends on the solvent, even though it is a π–π* excitation. As shown in Table 1, the absorption energy in 1,4-dioxane is 3.73 eV, while that in water solution is 3.38–3.35 eV. On the other hand, other absorption peaks are almost insensitive to the solvent.

Considering the properties of the solvents, there are two reasons for the red shift. The first is the dielectric polarization of the solvent due to the charge distribution of the solute. Table 1 also shows the dielectric constant of the solvent. The magnitude of the red shift tends to be greater if the dielectric constant of the solvent is larger. The second reason is hydrogen bonding between LF and the solvent. In protic solvents as H_2O and MeOH, the absorption maximum shifts to lower energy.

We estimated the absorption energy in water solution as follows. In the first step, we performed the SAC-CI calculation using PCM. In the next step, the effects of the explicit solvent molecules were estimated using an ONIOM [34] -like approach. For this purpose, two types of CIS calculations were performed: one with PCM and the other with five explicit water molecules (Fig. 1b) and PCM. The change in excitation energy accounts for the correction introduced by the explicit solvent molecules, and is used as an energy correction to the SAC-CI + PCM excitation energy. The PCM calculation correctly reproduced the solvation effect in the π–π* transition. The explicit water model was therefore expected to improve the description of the n–π* transitions in water solution. The water molecules were placed at the protic part of LF, where the hydrogen bondings take place. The rest of the solvation effect was taken into account by PCM. To reduce the computing time and resources, the structure of the LF-water complex was kept to C_s symmetry. Since the hydrogen bonding effect is mainly electrostatic [35], this approximated model would be qualitatively correct enough to describe hydrogen bonding to the lone-pair electrons of the O and N atoms in LF.

The results are summarized in Table 1. The excitation energy of the $3^1A'$ state changes to 3.54 eV, which is a red shift of 0.30 eV compared to the gas-phase result. The deviation from the experimental peak position changes to 0.16–0.19 eV. On the other hand, the solvation effect on the $2^1A'$ state was estimated

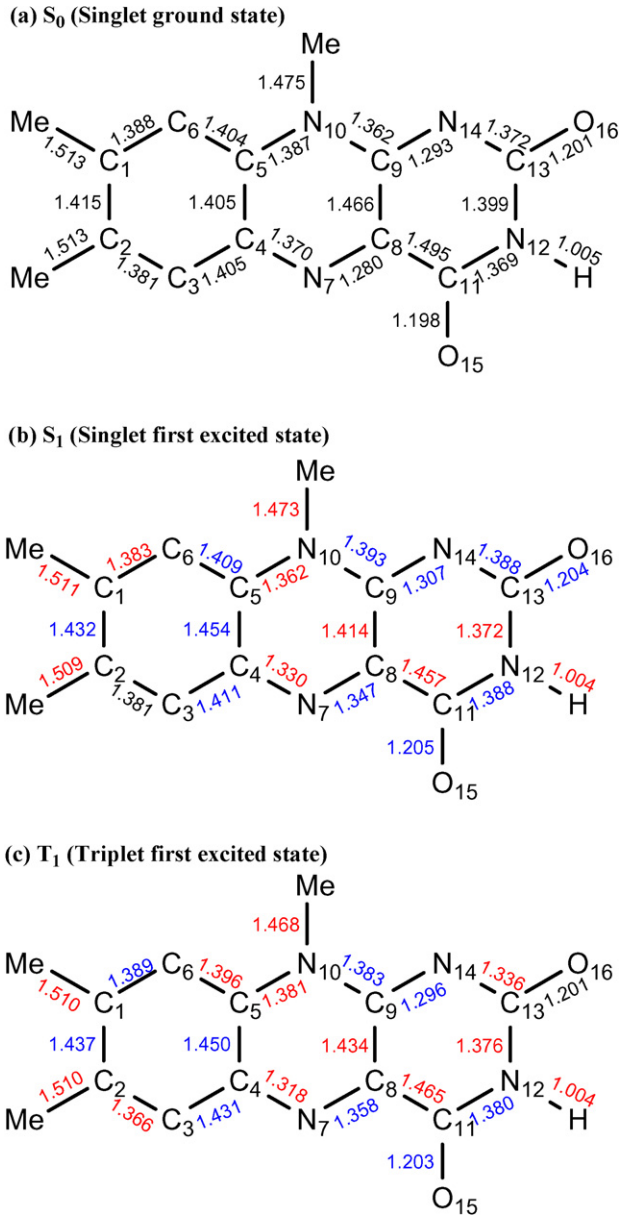

Fig. 3. SAC/SAC-CI optimized structures of S_0 (singlet ground), S_1 (singlet first excited) and T_1 (triplet first excited) states of lumiflavin. Compared to the S_0 state, longer and shorter bonds are shown in blue and red, respectively. Bond-length deviations greater than 0.03 Å are shown in bold face.

to be a red shift of only 0.06 eV, which agrees with the trend in the experiment [8]. The $4^1A'$ and $5^1A'$ states also show only small solvatochromism.

The solvation effects in the n–π* transitions tend to be greater than that in the π–π* transitions. The excitation energies of the $1^1A''$ and $2^1A''$ states in water solution were estimated to be 3.28 and 4.05 eV, respectively. These results involve a blue shift of 0.10 and 0.46 eV, respectively, compared to the gas-phase result. In particular, the $2^1A''$ state showed marked blue shift. One reason is in the orbital distribution of the 62th MO. The wave function of the $2^1A''$ state is one electron transition from 62th MO to 68th MO. As clearly seen in Fig. 2, the 62th MO distributes over the right hand of the molecule. On the other hand, the $3^1A'$ state shows red shift in water solution and is one electron transition from 66th MO. The distribution of the 66th MO is in the left side of LF. Since direction of the dipole moments of the two states were opposite, the solvatochromic shift of the $2^1A''$ state is also opposite to that of the $3^1A'$ state.

To qualitatively analyze the solvatochromic shift, we performed a series of CI-Singles calculations using different environments. First, the shift due to direct hydrogen bonding was estimated by the excitation energy difference between the explicit solvation model (W) and the gas phase model (*G*), which are listed in the "$E_{ex}(W) - E_{ex}(G)$" column in Table 3. Second, the dielectric polarization effect of the solvent was estimated by the excitation energy difference between the W plus PCM model and the W model, which are summarized in the "$E_{ex}(W+P) - E_{ex}(W)$" column. The total solvatochromism shift, $E_{ex}(W+P) - E_{ex}(G)$, is also listed.

As shown in Table 3, the explicit solvation effect and the dielectric polarization of the solution contribute almost equally to the total solvatochromic shift in the $3^1A'$ state. This result could be interpreted in terms of the MO populations. The $3^1A'$ state arises from a transition from HOMO-1 to LUMO. HOMO-1 has a population localized in the left ring. Consequently, the dipole moment of the state increases more than those of the ground and the $2^1A'$ states, as shown in Table 2. This increase in the solute dipole causes dielectric stabilization of the solvent. In HOMO-1, there is little amplitude in the N14 and O16 atoms, which are supposed to be the hydrogen bond acceptors. Since negative charges on the N14 and O16 atoms increase upon excitation, direct hydrogen bonds contribute to the red shift of the excitation energy.

Table 3
Solvent effect to the excitation energy calculated by CI-Singles with several solvation models

State	Gas phase	Five water molecules (W)		W plus PCM (W + P)		Total	PCM only	
	$E_{ex}(G)$	$E_{ex}(W)$	$E_{ex}(W) - E_{ex}(G)$	$E_{ex}(W+P)$	$E_{ex}(W+P) - E_{ex}(W)$	$E_{ex}(W+P) - E_{ex}(G)$	$E_{ex}(P)$	$E_{ex}(W+P) - E_{ex}(P)$
π–π* transitions								
$2^1A'$	4.29	4.23	−0.06	4.14	−0.09	−0.15	4.16	−0.02
$3^1A'$	5.14	5.02	−0.12	4.90	−0.12	−0.24	4.92	−0.02
$4^1A'$	6.04	5.98	−0.06	5.93	−0.05	−0.11	5.94	−0.01
$5^1A'$	6.66	6.64	−0.02	6.61	−0.03	−0.05	6.62	−0.01
n–π* transitions								
$1^1A''$	4.71	4.69	−0.02	4.77	0.08	0.06	4.87	−0.10
$2^1A''$	5.71	5.88	0.17	6.10	0.22	0.39	6.17	−0.07

In the excited states of LF, direct hydrogen bonds and dielectric polarization of solution contribute equally to the total solvatochromic shift. Therefore, both the explicit solvating molecules and PCM are necessary to quantitatively describe the solvation effect of water. If we only use PCM ("P" in Table 3), the result for the π–π* state is very close to that for the W + P model. In the PCM model, charges relevant to the electron density of the solute are generated on the surface of the cavity [18]. These surface charges might help the PCM to describe the microscopic solvation effect. However, this P model gives deviations of 0.10 and 0.07 eV in the n–π* states.

4. Conclusion

The excited states of LF were studied by the SAC-CI method. Considering the solvation effect on the absorption peaks, we obtained theoretical assignment for the experimental absorption peaks below 5 eV. Transition energies of two n–π* states were calculated at 3.3 and 4.1 eV. The molecular structures of the first singlet and triplet excited states were optimized using the SAC-CI method. The structural changes observed upon transitions were at most 0.05 Å. The solvation effect on the absorption energy was investigated by PCM and by including explicit water molecules. The characteristic solvatochromism observed for the second π–π* transition was analyzed. Both direct hydrogen bonding and dielectric polarization effects are responsible for the red shift in the $3^1A'$ state. Both effects were equally important in all the states investigated. If the solvation effect is described only by the PCM (P model), the absorption energies calculated for π–π* states were very close to those obtained with the PCM plus explicit water molecules model (the W + P model). However, in the case of the n–π* states, the results were overestimated by 0.07–0.10 eV. This indicates that the results would be more reliable to include hydrogen bonding effect in addition to the PCM.

Acknowledgement

This study was supported by a Grant-in-Aid for Creative Scientific Research and for Young Scientists from the Ministry of Education, Culture, Sports, Sciences, and Technology of Japan. The authors thank RCCS (Okazaki) and KUDPC (Kyoto) for computing time.

References

[1] D. Voet, J. Voet, Biochemistry, 2nd ed., John Wiley & Sons, New York, 1995.
[2] M. Sun, P.S. Song, Biochemistry 12 (1973) 4663.
[3] T. Climent, R. González-Luque, M. Merchán, L. Serrano-Andrés, J. Phys. Chem. A 110 (2006) 13584.
[4] A.M. Edwards, C. Bueno, A. Saldaño, E. Silva, K. Kasssab, L. Polo, G. Jori, J. Photochem. Photobiol. 48 (1999) 36.
[5] M. Meyer, H. Hartwig, D. Schomburg, J. Mol. Struct. (THEOCHEM) 364 (1996) 139.
[6] C. Neiss, P. Saalfrank, M. Parac, S. Grimme, J. Phys. Chem. A 107 (2003) 140.
[7] M. Sikorski, E. Sikorska, A. Koziolowa, R.G. Moreno, J.L. Bourdelande, R.P. Steer, F.J. Wilkison, Photochem. Photobiol. B: Biol. 60 (2001) 114.
[8] E. Sikorska, I.V. Khmelinskii, W. Prukala, S.L. Williams, M. Patel, D.R. Worrall, J.K. Bourdelande, J. Koput, M. Sikiorski, J. Phys. Chem. A 108 (2004) 1501.
[9] E. Sikorska, I. Khemelinskii, J. Koput, M. Sikorski, J. Mol. Struct. (THEOCHEM) 155 (2004).
[10] E. Sikorska, I. Khemelinskii, A. Komasa, J. Koput, L.F.V. Ferreira, J.R. Herance, J.L. Bourdelande, S.L. Williams, D.R. Worrall, M. Insińska-Rak, M. Sikorski, Chem. Phys. 314 (2005) 239.
[11] E. Sikorska, J.R. Herance, J.L. Bourdelande, I.V. Khmelinskii, S.L. Williams, D.R. Worrall, G. Nowacka, A. Komosa, M. Sikiorski, J. Photochem. Photobiol. A: Chem. 170 (2005) 267.
[12] H. Nakatsuji, K. Hirao, J. Chem. Phys. 68 (1978) 2053.
[13] H. Nakatsuji, Chem. Phys. Lett. 59 (1978) 362.
[14] H. Nakatsuji, Chem. Phys. Lett. 67 (1979) 329.
[15] H. Nakatsuji, Chem. Phys. Lett. 67 (1979) 334.
[16] H. Nakatsuji, in: J. Leszczynski (Ed.), Computational Chemistry—Reviews of Current Trends, vol. 2, World Scientific, Singapore, 1997, p. 62.
[17] M. Ehara, J. Hasegawa, H. Nakatsuji, in: C. Dykstra, G. Frenking, K. Kim, G. Scuseria (Eds.), Theory and Applications of Computational Chemistry: The First Forty Years, Elsevier Science, 2005.
[18] J. Tomasi, M. Persico, Chem. Rev. 94 (1994).
[19] J. Tomasi, R. Cammi, B. Mennucci, Int. J. Quant. Chem. 75 (1999) 783.
[20] V. Barone, M. Cossi, J. Tomasi, J. Comp. Chem. 19 (1998) 404.
[21] P. Hohenberg, W. Kohn, Phys. Rev. 136 (1964) B864.
[22] W. Kohn, L.J. Sham, Phys. Rev. 140 (1965) A1133.
[23] R.G. Parr, W. Yang, Density-Functional Theory of Atoms and Molecules, Oxford Univ. Press, Oxford, 1989.
[24] C. Lee, W. Yang, R.G. Parr, Phys. Rev. B 37 (1988) 785.
[25] A.D. Becke, J. Chem. Phys. 98 (1993) 5648.
[26] J. Rodríguez-Otero, M.-N.E.A. Peña-Gallego, S.A. Vázquez, J. Org. Chem. 67 (2002) 6347.
[27] W.J. Hehre, R. Ditchfield, J.A. Pople, J. Chem. Phys. 56 (1972) 2257.
[28] P.C. Hariharan, J.A. Pople, Theor. Chim. Acta 28 (1973) 213.
[29] T.H. Dunning_JR, P.J. Hay, in: H.F. Schaefer III (Ed.), Methods of Electronic Structure Theory, Prenum Press, New York, 1977.
[30] H. Nakatsuji, Chem. Phys. 75 (1983) 425.
[31] M.J. Frisch, G.W. Trucks, H.B. Schlegel, G.E. Scuseria, M.A. Robb, J.R. Cheeseman, J.J.A. Montgomery, T. Vreven, K.N. Kudin, J.C. Burant, J.M. Millam, S.S. Iyengar, J. Tomasi, V. Barone, B. Mennucci, M. Cossi, G. Scalmani, N. Rega, G.A. Petersson, H. Nakatsuji, M. Hada, M. Ehara, K. Toyota, R. Fukuda, J. Hasegawa, M. Ishida, T. Nakajima, Y. Honda, O. Kitao, H. Nakai, M. Klene, X. Li, J.E. Knox, H.P. Hratchian, J.B. Cross, C. Adamo, J. Jaramillo, R. Gomperts, R.E. Stratmann, O. Yazyev, A.J. Austin, R. Cammi, C. Pomelli, J.W. Ochterski, P.Y. Ayala, K. Morokuma, G.A. Voth, P. Salvador, J.J. Dannenberg, V.G. Zakrzewski, S. Dapprich, A.D. Daniels, M.C. Strain, O. Farkas, D.K. Malick, A.D. Rabuck, K. Raghavachari, J.B. Foresman, J.V. Ortiz, Q. Cui, A.G. Baboul, S. Clifford, J. Cioslowski, B.B. Stefanov, G. Liu, A. Liashenko, P. Piskorz, I. Komaromi, R.L. Martin, D.J. Fox, T. Keith, M.A. Al-Laham, C.Y. Peng, A. Nanayakkara, M. Challacombe, P.M.W. Gill, B. Johnson, W. Chen, M.W. Wong, C. Gonzalez, J.A. Pople, Gaussian Development Version, Revision B. 04., Gaussian, Inc., Pittsburgh, PA, 2003.
[32] W.A. Eaton, J. Hofrichter, M.W. Makinen, R.D. Andersen, M.L. Ludwig, Biochemistry 14 (1975) 2146.
[33] L.B.A. Johansson, A. Davidsson, G. Lindblom, K.R. Naqvi, Biochemistry 18 (1979) 4249.
[34] F. Maseras, K. Morokuma, J. Comp. Chem. 16 (1995) 1170.
[35] K. Morokuma, Acc. Chem. Res. 10 (1977) 294.